

## Shape Coexistence and Electric Monopole Transitions in $^{184}\text{Pt}$

Y. Xu, K. S. Krane, and M. A. Gummin

*Department of Physics, Oregon State University, Corvallis, Oregon 97331*

M. Jarrio and J. L. Wood

*School of Physics, Georgia Institute of Technology, Atlanta, Georgia 30332*

E. F. Zganjar

*Department of Physics and Astronomy, Louisiana State University, Baton Rouge, Louisiana 70803*

H. K. Carter

*UNISOR, Oak Ridge Associated Universities, Oak Ridge, Tennessee 37831*

(Received 13 February 1992)

Levels in  $^{184}\text{Pt}$  were studied from the decay of mass-separated  $^{184}\text{Au}$  by gamma-ray and conversion-electron spectroscopy and by gamma-ray angular distributions from low-temperature nuclear orientation. In addition to coexisting  $K^\pi=0^+$  bands, coexisting  $K^\pi=2^+$  bands are observed at low energy. Strong interband electric monopole transitions are observed between states of the two  $K^\pi=0^+$  bands and also between states of the two  $K^\pi=2^+$  bands. The coexistence of  $K^\pi=2^+$  bands at low energy represents a new type of collective structure.

PACS numbers: 23.20.Lv, 23.20.En, 23.20.Nx, 27.70.+q

Shape coexistence is widely manifested [1] in nuclei. A dramatic example occurs in the neutron-deficient Hg ( $Z=80$ ) isotopes, where weakly deformed oblate and strongly deformed prolate shapes coexist at low energy [2,3]. We report details here of coexisting shapes at low energy in  $^{184}\text{Pt}$  ( $Z=78$ ) with a completely new feature: In addition to two bands of states with  $I^\pi=0^+, 2^+, 4^+, 6^+$  ( $K^\pi=0^+$  bands), we observe two bands of states with  $I^\pi=2^+, 3^+, 4^+$  ( $K^\pi=2^+$  bands). These two  $K^\pi=2^+$  bands, which occur at low excitation energy, are connected by strong electric monopole ( $E0$ ) transitions. The association of  $E0$  transitions with shape coexistence is well recognized [4] but has previously been established only in the case of  $K^\pi=0^+$  bands; here we report that  $E0$  transitions are also associated with coexistence of  $K^\pi=2^+$  bands.

Excited states of  $^{184}\text{Pt}$  were studied through the radioactive decay of mass-separated  $^{184}\text{Au}$  ( $t_{1/2}=53$  s,  $I=6$ ) by using the UNISOR isotope separator operated on line [5] to the 25-MV folded tandem accelerator at the Holifield Heavy-Ion Research Facility (HHIRF). The  $^{184}\text{Au}$  was produced through the  $(^{12}\text{C}, 9n)$  reaction on a target of  $^{181}\text{Ta}$  using a beam of 140-MeV  $^{12}\text{C}$  ions. Gamma-ray and conversion-electron (ce) spectrum multi-scaling and  $\gamma$ - $\gamma$ - $t$ , and  $\gamma$ - $x$ - $t$ ,  $\gamma$ -ce- $t$ , and ce- $x$ - $t$  coincidence measurements were conducted on line. Conversion-electron spectra were taken with a  $200\text{ mm}^2 \times 3\text{ mm}$  cooled Si(Li) detector. All assignments of  $\gamma$ -ray and internally converted transitions were made on the basis of coincidence information.

In a separate experiment, angular distributions of the  $\gamma$  rays were measured following the decay of  $^{184}\text{Au}$  oriented at low temperatures. The nuclei were produced using the same reaction as the spectroscopy experiment. The ac-

tivity was mass separated on line in the UNISOR separator and then transported to the UNISOR Nuclear Orientation Facility [6], a  $^3\text{He}$ - $^4\text{He}$  dilution refrigerator that is on line to the mass separator. The radioactive nuclei were implanted at 50 kV into a polarized Fe target in the refrigerator, which operates at a temperature below 7 mK with beam on target. The angular distributions of the  $\gamma$  rays were observed with an array of six Ge detectors surrounding the target at a distance of about 10 cm.

The  $^{184}\text{Au}$  decay scheme is exceedingly complex; in total we have assigned more than 150  $\gamma$  transitions and have established 52 levels in  $^{184}\text{Pt}$ . Here we discuss only the low-lying levels shown in Fig. 1; a more complete level scheme will be published [7] elsewhere. Some of the levels shown in Fig. 1 are also seen by in-beam work [8]. The two coexisting  $0^+$  bands can be seen clearly in the scheme shown in Fig. 1. The lower band is the more strongly deformed, as can be seen from the energy spacing. This is consistent with the calculations of Bengtsson *et al.* [9], which show pronounced minima in the potential energy surface for  $^{184}\text{Pt}$  corresponding to a prolate ground state with deformation parameter  $\beta=+0.22$  and an oblate excited band with  $\beta=-0.16$  at an excitation of about 500 keV. By fitting the energies of the high-spin members of the ground band to the rotational formula with higher-order terms, Dracoulis *et al.* [10] studied the perturbation of the energies due to the mixing of the two bands and concluded that the mixing is near maximal, the unperturbed bandheads are separated by only 50 keV (vs 500 keV for the perturbed states), the interaction strength is 250 keV, and the rotational parameters for the two bands are 15 and 50 keV. If this hypothesis about the mixing is correct, the two bands should [11,12] be connected by  $\Delta I=0$  transitions with substantial  $E0$  com-

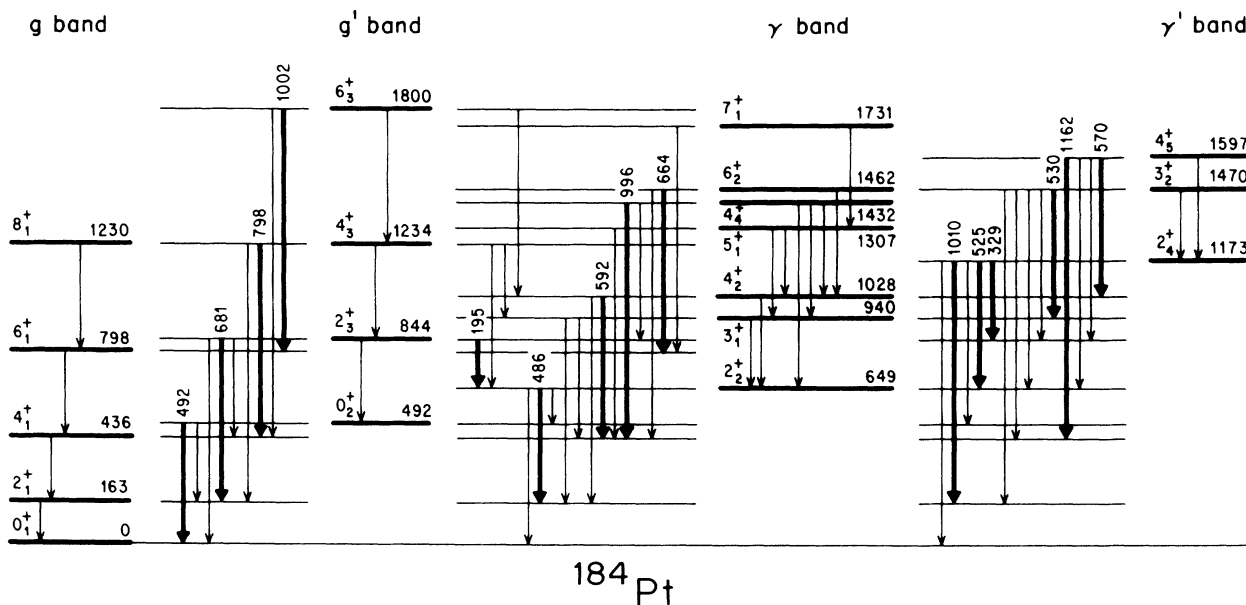


FIG. 1. The low-lying levels of  $^{184}\text{Pt}$ . Thick lines indicate  $\Delta I=0$  transitions. The  $g$ ,  $g'$ ,  $\gamma$ , and  $\gamma'$  bands built on the ground state and 492-, 649-, and 1149-keV excited states, respectively, are separated. The  $2_1^+$ ,  $4_1^+$ ,  $6_1^+$ ,  $8_1^+$ ,  $2_3^+$ ,  $4_3^+$ ,  $5_1^+$ , and  $7_1^+$  states have been seen by in-beam spectroscopy [8]. The  $4_4^+$ ,  $5_1^+$ ,  $6_2^+$ , and  $7_1^+$  states associated with the  $\gamma$  band are not discussed here, but they are shown for completeness.

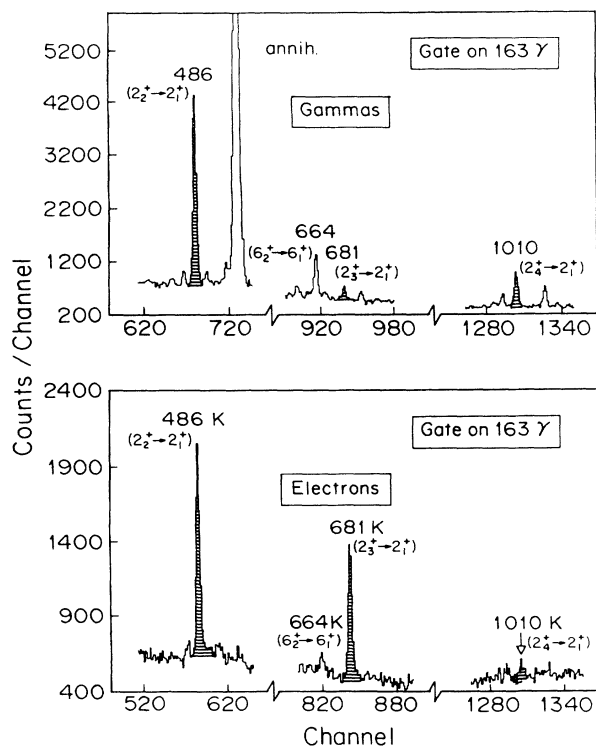


FIG. 2. Portions of gamma (top panel) and electron (bottom panel) spectra in coincidence with the 163-keV ( $2_1^+ \rightarrow 0_1^+$ ) transition. Note the enhancement of the conversion of the 681-keV ( $2_3^+ \rightarrow 2_1^+$ ) transition relative to that of the 486-keV ( $2_2^+ \rightarrow 2_1^+$ ) and 1010-keV ( $2_4^+ \rightarrow 2_1^+$ ) transitions.

ponents competing successfully with the  $M1+E2$  multipoles. The  $E0$  strength is proportional to the mixing amplitudes and to the difference in mean-square radii (or, equivalently, deformation parameters) of the two bands. The observation of  $E0$  transitions in competition with  $M1$  and  $E2$  transitions serves as a definitive test of the interpretation of the level structure described above. Figure 2 shows portions of the spectrum of the gamma rays and conversion electrons gated on the 163-keV ( $2_1^+ \rightarrow 0_1^+$ ) transition. Lines can be seen corresponding to three transitions that proceed from higher-lying  $2^+$  states to the first excited state. In one case (681 keV) the electron intensity is anomalously large compared with the gamma intensity; this large electron intensity signals the  $E0$  component and marks this transition as connecting the coexisting bands.

A unique feature of the  $^{184}\text{Pt}$  level scheme is the *second* set of coexisting bands, built on the  $2^+$  states of 649 and 1173 keV. Confirmation of this identification can be found in the  $E0$  transitions connecting the bands. Figure 3 compares the coincidence-gated gamma and electron spectra in the region of the 525-keV transition, which connects the  $2^+$  bandheads. The electron intensity of the 525-keV transition is anomalously large compared with that of the 586-keV  $E2$  transition. An extreme example of this effect is also shown in Fig. 4 for the case of the 530-keV ( $3_2^+ \rightarrow 3_1^+$ ) transition; in this case a strong electron line is seen, but the corresponding gamma line is not seen at all.

Table I summarizes the properties of the  $\Delta I=0$  transi-

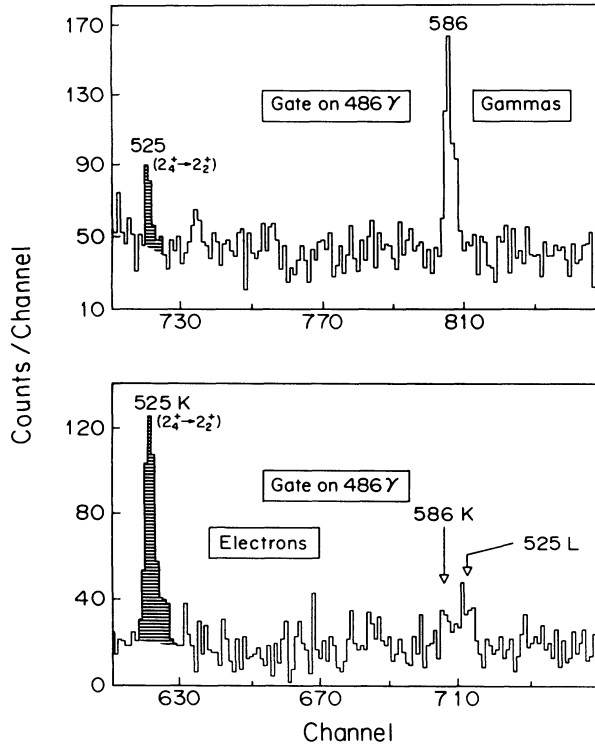


FIG. 3. Portions of the gamma (top panel) and electron (bottom panel) spectra in coincidence with the 486-keV ( $2_2^+ \rightarrow 2_1^+$ ) transition. Note the enhancement of the conversion of the 525-keV transition relative to the 586-keV  $E2$  transition.

tions observed in the present work. The anomalously large conversion coefficients of certain of these transitions are immediately obvious from this tabulation by virtue of their large values of the ratio  $\alpha_K(\text{expt})/\alpha_K(M1)$ , which clearly single out those transitions connecting the coexisting configurations. To make this argument more quantitative, it is necessary to extract the relative  $E0$  admixtures in the transitions, which requires knowledge of the relative amount of  $M1$  and  $E2$  radiations present in these  $\Delta I=0$  transitions. For this determination we have measured the gamma-ray angular distributions from  $^{184}\text{Au}$  oriented at low temperature. We have analyzed the anisotropies of the transitions connecting the levels in Fig. 1 in such a way that the results are independent of any uncertainties resulting from the complex feeding of these levels from higher-lying states. From the analysis of the angular distributions, we have determined  $E2/M1$  mixing ratios for many of the transitions. Knowledge of the conversion coefficients (corresponding to  $E0+M1+E2$ ) and the  $E2/M1$  mixing ratios then permits the relative amounts of  $E0$ ,  $M1$ , and  $E2$  radiations to be determined. These values are given in Table I in terms of the percentage of each multipole relative to the total transition intensity (all multipoles of gammas and electrons).

A further insight to these coexisting structures can be gained by estimating the electric monopole transition

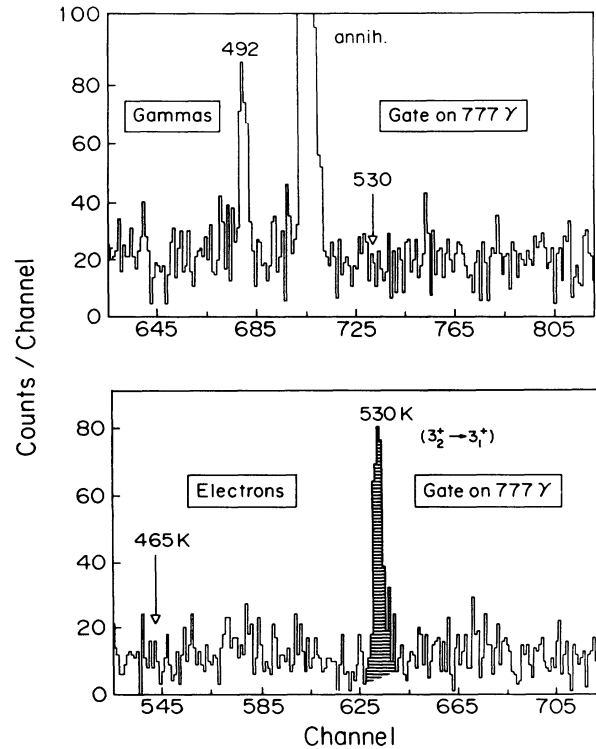


FIG. 4. Portions of the gamma (top panel) and electron (bottom panel) spectra in coincidence with the 777-keV ( $3_1^+ \rightarrow 2_1^+$ ) transition. Note the lack of a gamma line corresponding to the 530-keV transition. The label "465 K" indicates the location of a hypothetical  $K$  line that would give an  $L$  line at the energy corresponding to the 530  $K$  line. No such line is present, indicating that the 451-keV electron line must indeed be a  $K$  line.

strength. The only lifetime data for excited states of  $^{184}\text{Pt}$  are for the yrast band [13]. However, by assigning the average of the  $B(E2, 2_1^+ \rightarrow 0_1^+)$  values observed [14] in  $^{190-196}\text{Pt}$  as the value of  $B(E2, 2_3^+ \rightarrow 0_2^+)$  in  $^{184}\text{Pt}$ , i.e.,  $B(E2, 2_3^+ \rightarrow 0_2^+) = 0.30 e^2 b^2$  (estimated), we obtain [15]  $\rho^2(2_3^+ \rightarrow 2_1^+) \times 10^3 = 25$ . This is comparable to the strongest  $\rho^2(0_2^+ \rightarrow 0_1^+) \times 10^3$  reported in a recent compilation [12].

A new feature has been added to the subject of coexisting shapes in nuclei: In addition to coexisting  $K^\pi=0^+$  bands, coexisting  $K^\pi=2^+$  bands can occur at low excitation energy. We observe these coexisting  $K^\pi=2^+$  bands to be connected to each other by strong  $E0$  transitions. In particular, we observe  $E0$  transitions between the  $I^\pi=2^+$  members of the two  $K^\pi=2^+$  bands but not between these  $I^\pi=2^+$  states and the  $2^+$  states of the  $K^\pi=0^+$  bands; that is, we observe strong  $E0$  components in the  $2_3^+ \rightarrow 2_1^+$  and  $2_4^+ \rightarrow 2_2^+$  transitions and no  $E0$  components in the  $2_2^+ \rightarrow 2_1^+$ ,  $2_3^+ \rightarrow 2_2^+$ ,  $2_4^+ \rightarrow 2_1^+$ ,  $2_4^+ \rightarrow 2_3^+$  transitions (Table I and Fig. 1). Further, the  $I^\pi=3^+$  members of the two  $K^\pi=2^+$  bands are connected only by an  $E0$  transition; no  $\gamma$ -ray transition is observed

TABLE I. Low-lying  $\Delta I = 0$  transitions in  $^{184}\text{Pt}$ .

Assignment <sup>a</sup>		$E_\gamma(\text{keV})$	$\alpha_K(\text{expt.})$	Theory <sup>b</sup>		$\frac{\alpha_K(\text{expt.})}{\alpha_K(\text{M1, th.})}$	%E0	%M1	%E2
$I_i \rightarrow I_f$				$\alpha_K(\text{M1})$	$\alpha_K(\text{E2})$				
$0_2 \rightarrow 0_1$	$g' \rightarrow g$	492	> 5.3	0.071	0.019	> 75			
$2_2 \rightarrow 2_1$	$\gamma \rightarrow g$	486	0.051(5)	0.073	0.020	0.7(1)	0(1)	82(5)	18(4)
$2_3 \rightarrow 2_1$	$g' \rightarrow g$	681	0.30(3)	0.030	0.0095	10(1)	22(2)	$32^{+21}_{-29}$	$46^{+21}_{-29}$
$2_3 \rightarrow 2_2$	$g' \rightarrow \gamma$	195	0.9(3)	0.86	0.18	1.0(3)	< 15		
$2_4 \rightarrow 2_1$	$\gamma' \rightarrow g$	1010	0.012(4)	0.011	0.0044	1.1(4)	< 0.75		
$2_4 \rightarrow 2_2$	$\gamma' \rightarrow \gamma$	525	0.36(4)	0.060	0.017	6.0(7)	22(2)		
$2_4 \rightarrow 2_3$	$\gamma' \rightarrow g'$	329	0.19(5)	0.21	0.049	0.9(3)	< 12		
$3_2 \rightarrow 3_1$	$\gamma' \rightarrow \gamma$	530	> 0.4	0.058	0.016	> 7	> 24		
$4_2 \rightarrow 4_1$	$\gamma \rightarrow g$	592	0.022(3)	0.044	0.013	0.5(1)	0.3(3)	$17^{+29}_{-17}$	$82^{+29}_{-17}$
$4_3 \rightarrow 4_1$	$g' \rightarrow g$	798	0.045(6)	0.020	0.0069	2.3(3)	3.1(5)	$44^{+15}_{-11}$	$53^{+15}_{-11}$
$4_4 \rightarrow 4_1$	$\gamma \rightarrow g$	996	< 0.014	0.011	0.0044	< 1.3			
$4_5 \rightarrow 4_2$	$\gamma' \rightarrow \gamma$	570	0.078(16)	0.048	0.014	1.6(3)	2.8(13)		
$4_5 \rightarrow 4_1$	$\gamma' \rightarrow g$	1162	$\leq 0.006$	0.0078	0.0034	< 0.8			
$6_2 \rightarrow 6_1$	$\gamma \rightarrow g$	664	0.0126(14)	0.0324	0.010	0.39(4)	0.0(2)	51(8)	49(8)
$6_3 \rightarrow 6_1$	$g' \rightarrow g$	1002	0.011(4)	0.011	0.0044	1.0(4)	0.3(4)	$51^{+12}_{-10}$	$49^{+12}_{-10}$

<sup>a</sup>See Fig. 1.<sup>b</sup>H. Roesel *et al.*, At. Data Nucl. Data Tables **21**, 91 (1978).

between these states.

We are grateful to the staffs of UNISOR and HHIRF for their assistance. This work was supported in part by the U.S. Department of Energy under Contracts No. DE-FG06-87ER40345 (Oregon State), No. DE-FG05-87ER40330 (Georgia Tech), No. DE-FG05-84ER40159 (Louisiana State), and No. AC05-76OR00033 (UNISOR).

- [1] K. Heyde, P. van Isacker, M. Waroquier, J. L. Wood, and R. A. Meyer, Phys. Rep. **102**, 291 (1983).
- [2] J. H. Hamilton, P. G. Hansen, and E. F. Zganjar, Rep. Prog. Phys. **48**, 631 (1985).
- [3] M. O. Kortelahti, E. F. Zganjar, J. L. Wood, C. R. Bingham, H. K. Carter, K. S. Toth, J. H. Hamilton, J. Kormicki, L. Chaturvedi, and W. B. Newbolt, Phys. Rev. C **43**, 484 (1991).
- [4] E. F. Zganjar and J. L. Wood, Nucl. Phys. A **520**, 427c (1990).
- [5] E. H. Spejewski, R. L. Mlekodaj, and H. K. Carter, Nucl. Instrum. Methods **186**, 71 (1981).

- [6] I. C. Girit *et al.*, Hyperfine Interact. **43**, 151 (1988).
- [7] Y. Xu *et al.* (to be published).
- [8] M. P. Carpenter *et al.*, Nucl. Phys. A **513**, 125 (1990).
- [9] R. Bengtsson, T. Bengtsson, J. Dudek, G. Leander, W. Nazarewicz, and J. Zhang, Phys. Lett. **183**, 1 (1987).
- [10] G. D. Dracoulis, A. E. Stuchbery, A. P. Byrne, A. R. Poletti, S. J. Poletti, J. Gerl, and R. A. Bark, J. Phys. G **12**, L97 (1986).
- [11] J. Kantele, in *Heavy Ions and Nuclear Structure*, Proceedings of the XIV Summer School, Mikolajki, Poland, 1984, edited by B. Sikora and Z. Wilhelm (Harwood Academic, New York, 1984).
- [12] K. Heyde and R. A. Meyer, Phys. Rev. C **37**, 2170 (1988).
- [13] U. Garg *et al.*, Phys. Lett. B **180**, 319 (1986).
- [14] S. Raman, C. H. Malarkey, W. T. Milner, C. W. Nestor, Jr., and P. H. Stelson, At. Data Nucl. Data Tables **36**, 1 (1987).
- [15] This value of  $\rho^2(2_3^+ \rightarrow 2_1^+)$  is obtained from our measured branching ratios for the decay of the  $2_3^+$  state and the method (see Ref. [11]) and tables of J. Kantele, Nucl. Instrum. Methods Phys. Res., Sect. A **271**, 625 (1988).